

RESONANT AIR-COUPLED CAPACITIVE TRANSDUCERS WITH TRANSMITTING AND ISOLATING RAILS ON THE BACKPLATE

PACS REFERENCE: 43.38.Bs

Name: Leschka, S.; Pfeifer, G.
Institution: Dresden University of Technology, Institute of Acoustics and Speech Communication
Address: Helmholtzstraße 18
Town: 01062 Dresden
Country: Germany
Tel: +49 351 46 33 22 53
Fax: +49 351 46 33 70 91
Email: Stephan.Leschka@ias.et.tu-dresden.de

ABSTRACT

Resonant air-coupled capacitive transducers were set up in a frequency range of about 100 kHz. A network model, which already considers the inhomogeneous electrical field enables the calculation of the on-axis sound pressure depending on the transducer geometry, material parameter, and the electrical input conditions. The predicted sound pressure of transducers with isolating rails corresponds to the results of measurements. Caused by the metal-film-connection, transducers with metal backplates generate a higher sound pressure than the one with the model calculated. The paper gives details about the modification of the network model to explain this phenomenon.

INTRODUCTION

Applications of air-coupled capacitive ultrasonic transducers have been internationally published by many authors. In the frequency range above 1 MHz, micro-mechanical technologies are used [2] [3] to set up good reducible transducer arrays. In doing so the resonance in membranes consisting of stretched nitride layers is used. The membranes mass and its tension determine the resonance frequency. The evacuation [5] of the volume between the membrane and the backplate can be accomplished with this method as well.

Extensive researches of the so-called V-structures are available below 500 kHz. Hereby, a stretched membrane vibrates over a backplate with V-shaped grooves. In [4] and [11], the calculation of the resonance frequency of this kind of transducers is discussed. A theory that agrees with numerous experimental results is provided by [10]. These transducers feature a high sensitivity.

Using rectangular isolating rails [1] of 3.75 μm height on a metallic backplate, wide band transducers were set up. Their resonance is determined by the stiffness of the air layer between membrane and the backplate and the membrane tension. It is settled between 300 kHz and 500 kHz.

This paper deals with the assessment of output limits of air-coupled capacitive ultrasonic transducers in the frequency range of about 100 kHz by multi-stripe membrane transducers. Thus, the resonance mode [7] was chosen to optimally use the low energy density of the electrostatic field for a generation of the highest sound pressure possible. A network model [9] is utilised to calculate the sound pressure depending on the transducer geometry, the chosen membrane material, and the electrical input conditions. In [8] is shown, to what extent inhomogeneous electrical fields with the resulting inhomogeneous force fields are utilised using network models. Especially by using transmitting rails on the backplate, dominating sources of oscillation energy are situated between the rails top side and the membrane. The influence of the metal-film-

connection on the transfer behaviour of the transducer can be estimated having knowledge of network modelling.

CONSTRUCTION OF A MULTI-STRIPE MEMBRANE TRANSDUCER

The left part of Figure 1 shows the layout of the transducer. A stretched and on the upper side metallized Kapton membrane is placed on a stiff, transmitting and plane backplate. There are parallel and equidistant rails with a rectangular section at the top side of the backplate. They have a supporting function for the membrane, which consists of a $7\mu\text{m}$ thick up-sided metallized Kapton film. The stripe membrane visualised in the right part of Figure 1 is built by a membrane stretched over a neighbouring couple of rails.

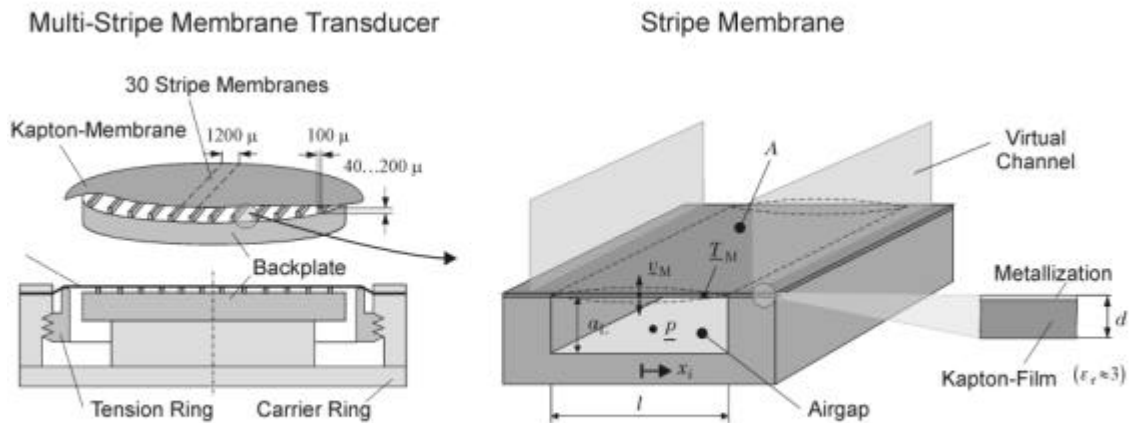


Figure 1 Left: Multi-Stripe Membrane Transducer, **Right:** Section of a Stripe Membrane

Except the border areas of the transducer, each of them has an in phase vibrating neighbour. Therefore the volume flux is charged in the virtual channel in front of the stripe membrane. The acoustic load rc results from it. The resonance frequency of each stripe membrane is determined by the rail distance l , the membrane tension T_M , its mass per area and the height of the airgap a_L . As the membrane vibrates in phase in direction of the rails, the analysis of the transverse section of one stripe membrane is representative for the whole multi-stripe membrane transducer.

NETWORK MODEL OF A STRIPE MEMBRANE

Figure 2 shows the network model of a stripe membrane whose derivation has already been discussed in [9].

The horizontal design of springs in the middle of Figure 2 describes the quasi static behaviour of the stretched membrane. The part of the membrane mass Dm is attached to each system point. It completes this part of the circuit to a waveguide, which correctly represents the stripe membrane at least including the first resonance. The acoustic level is in the upper part of Figure 2. It is required that the sound pressure is independent from the position on the membrane section. The result of this is the outlet-sided parallel connection of the surface transformer. Each surface transformer (Y) converts the membrane velocity \underline{v}_j in the volume flux \underline{q}_j . The electrical power is input by the sources E_j shown in the lower part of Figure 2. The resonance mode is chosen to optimally utilize the energy of the propulsive electrical field for the sound generation. With the existing ratio of membrane movement to rail height smaller than 5%, the negative spring elements resulting from the effects of an electrical field can be neglected.

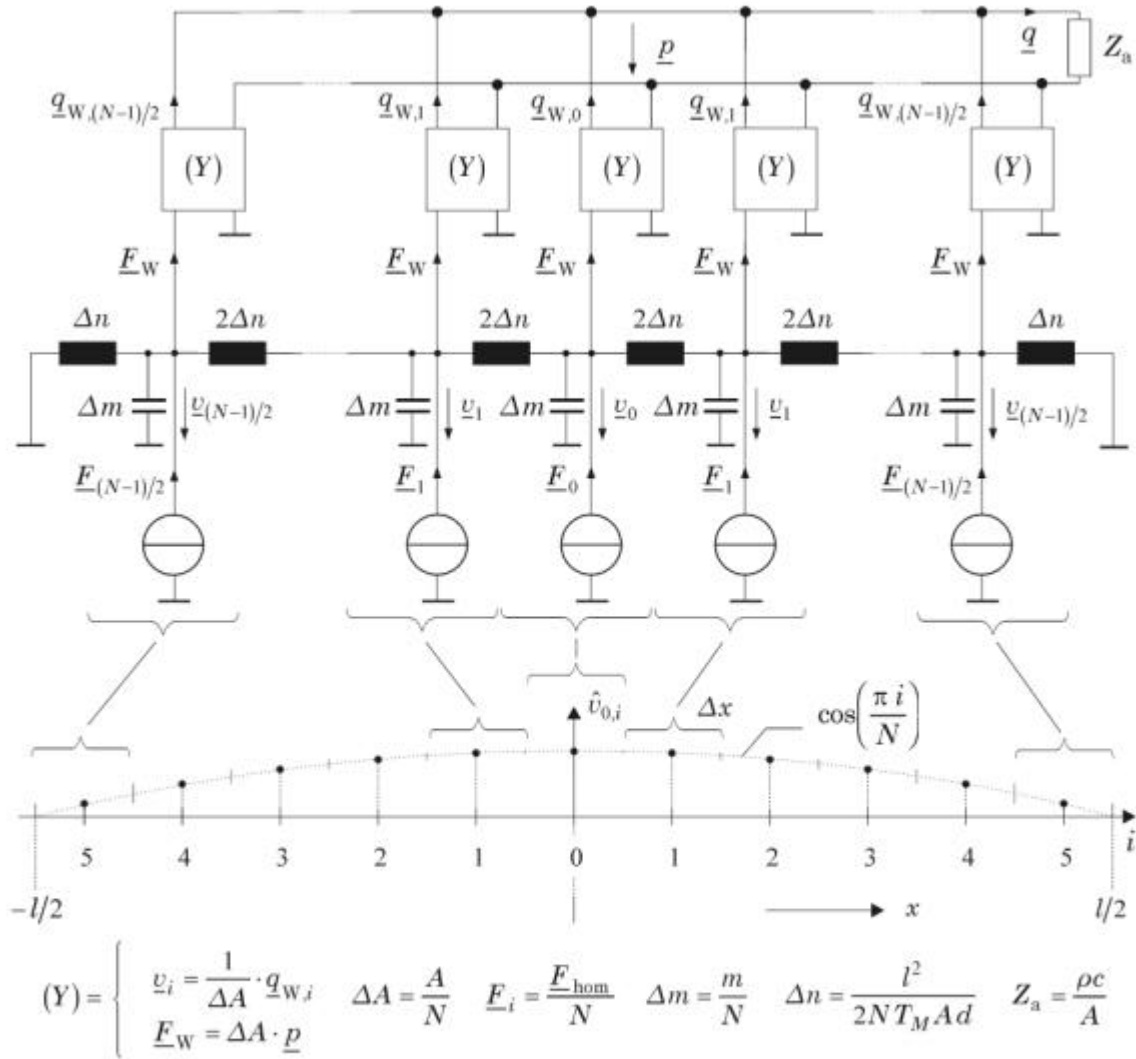


Figure 2 Top: Network Model of a Stripe Membrane, **Bottom:** Velocity in the Centre of the Stripe Membrane Caused by a Single Force F_i

MEMBRANE VELOCITY IN RESONANCE MODE

A membrane velocity v_0 in the middle of the stripe membrane results from the input of the first harmonic component of the homogenous electrical force in the network model:

$$F_{\text{hom}}(\omega) = \frac{\epsilon_0 \bar{U} U(\omega) A}{\left(a_L + \frac{d}{\epsilon_r} \right)^2} \quad (1)$$

The homogenous mechanic-acoustical transfer factor gives the ratio of both parameters in the resonance mode:

$$H_{\text{hom}} = \frac{v_0}{F_{\text{hom}}}|_{A=1\text{m}^2} = 3.8 \frac{\text{mm}}{\text{Ns}} \quad (2)$$

Without loss of generality, a membrane surface area of 1m^2 can be assumed, as any stripe membrane can have any length in direction of the rails. Under this stimulation, the membrane

vibrates in its cosine eigen mode, which is also retained under an inhomogeneous force distribution. The diagram in the lower part of Figure 2 shows the effect that each single power F_i has on the membrane velocity in the membrane centre. Thus, each local single force is weighted with the eigen mode of the membrane. The zones of high impedance near the rails only have a small share of the generation of the membrane velocity. Any inhomogeneous force distribution over the section of the stripe membrane can be split to the corresponding power F_i .

Regarding multi-stripe membrane transducers with transmitting and isolating rails, the calculated and measured velocity of the equivalent piston transducer will be confronted. The equivalent piston velocity \hat{v}_p is proportional to the maximum sound pressure which appears dependent on the frequency and the transducer diameter on the transducers principal axis.

In the theoretical curves calculated with the network model the discussed compression loss [9] by heat conduction [6] are considered in the transducer airgaps. They increase the acoustical load.

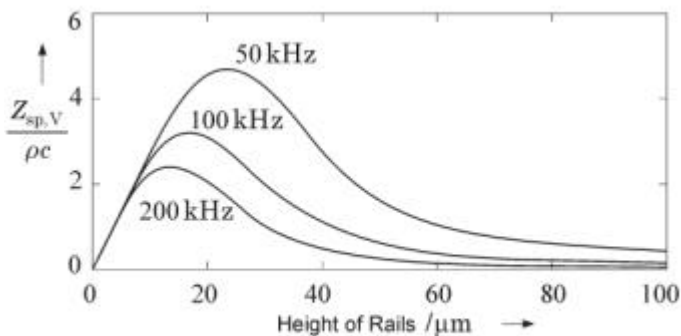


Figure 3: Compression Loss Caused by Heat Conduction

As in Figure 3 visualised, these compression loss $Z_{sp,V}$ is standardised for the load of the sound field for three frequencies. The compression loss can only be minimised for very small (isothermal marginal value) or very high (adiabatical marginal value) rails. The maximal compression loss having a frequency of 100 kHz is reached with a rail height of 15 μm . The compression loss decreases under the load of the sound field for rail heights bigger than 40 μm .

Small rail heights below 5 μm have low compression loss as well. Caused by unavoidable tolerances resulting from the distance between membrane and backplate, the resonance frequencies vary locally a lot. Thus, such transducers are broadbanded. Hence, multi-stripe membrane transducers with rail heights between 40 μm and 200 μm have been analysed to utilise the resonance effect.

Multi-stripe membrane transducers with isolating rails made of solder resist have an almost homogeneous electrical field in the airgap. The calculated and measured velocity of the equivalent piston shown in Figure 4 matches well in the areas of low input voltages. The dots marked by transgression of the disruptive strength in the corner between membrane

Multi-Stripe Membrane Transducers with Isolating Rails made of solder resist have an almost homogeneous electrical field in the airgap. The calculated and measured velocity of the equivalent piston shown in Figure 4 matches well in the areas of low input voltages. The dots marked by transgression of the disruptive strength in the corner between membrane

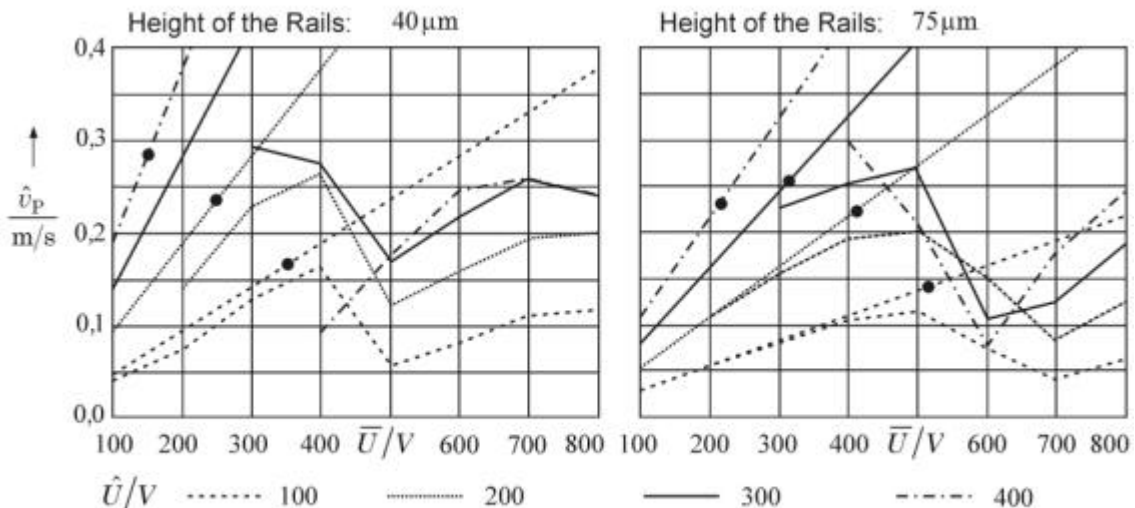


Figure 4: Multi-Stripe Membrane Transducer with Isolating Rails, Velocity of the Equivalent Piston Transducer, Theorie (Straight Line) and Microphone Measurement

and backplate limits this transducer principle. Caused by this effect, the field strength in the homogeneous part of the airgap does not reach the disruptive strength expected under this rail height. The reason is that the airgap is ionised prematurely by the effect in the corner.

Multi-Stripe Membrane Transducers with transmitting Rails. The inhomogeneous electrical field in the airgap causes high forces near the transmitting rails made of brass. The resulting inhomogeneous force distribution $\vec{F}_i(x_i)$ was calculated with a field simulation and included in the network model. Thereby, the membrane velocity slightly increases compared with its value caused by a homogeneous electrical field (factor 1.5 for 200 μm height of rails). As it can be seen in Figure 5, the measured sound pressure in the area of small compression loss in the airgap is almost independent of the rail height.

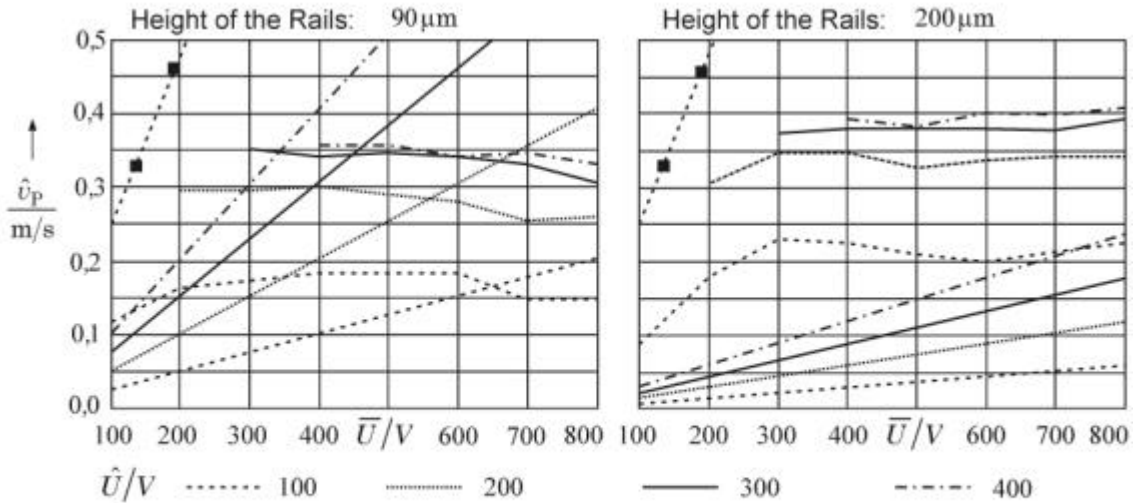


Figure 5: Multi-Stripe Membrane Transducer with Transmitting Rails, Velocity of the Equivalent Piston Transducer, Theorie (Straight Line) and Microphone Measurement, **Each Left Top:** Theoretical Straight Lines Considering Metal-Film-Connection

This effect considering the homogeneous and inhomogeneous electrical field in the airgap is not explainable. The disruptive strength in the corner between rails and membrane is exceeded using voltages of around 20 V. Thus, a premature ionisation of the airgap is assumed. The achieved membrane velocity, especially under low voltages can not be explained considering the homogeneous and inhomogeneous fields in the airgap between membrane and backplate.

Considering the metal-film-connection. There are vibratory membrane parts over the rails, because of the waviness of the membrane film on a rail topside. After equation 1 with $a_L \rightarrow 0$, in the zones of high impedance, a few decades higher dynamic forces are input in the membrane rather than in the area of the airgap between the membrane and the backplate.

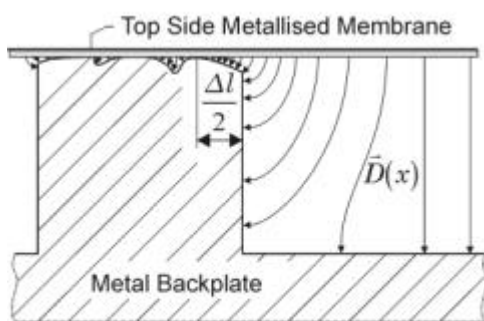


Figure 6: Metal-Film-Connection

The metal-film-connection results from the statistically generated contact surfaces between the rail topside and the membrane. It inputs energy in the uncommitted vibrating membrane in the regions between rail edge up to the first support point of the membrane on the rail topside. This zone in comparison to the rail distance is very small. As illustrated in Figure 6, the distance of supporting points of the membrane on the rails increases from the rail distance l to $l+2\Delta l/2$.

A very dense position of the power source in the network model would be needed to get the right effect of this part of force between rail topside and membrane up to the supporting points. Thus, it is easier to utilise the knowledge about the local assessment of the force field $\vec{F}_i(x_i)$ caused by the eigen mode of the membrane, which is gained from the network model and visualised in Figure 2. The homogeneous mechanical-acoustic transfer factor being applied in equation 2 raises by the form factor \tilde{I} including the metal-film-connection. This factor is seen in equation 3:

$$\bar{I} = \frac{\pi}{2} \sum_{x_i = -(l+\Delta l)/2}^{(l+\Delta l)/2} I(x_i) \cos\left(\frac{\pi x_i}{l+\Delta l}\right) \frac{\Delta x_i}{l+\Delta l} \quad \text{mit} \quad I(x_i) = \frac{\hat{F}(x_i)}{\hat{F}_{\text{hom}}(x_i)} \quad (3)$$

$$\hat{F}(x_i) = \begin{cases} \text{field simulation} & |x_i| < l/2 \\ \text{Gl (1)} \cdot \frac{\Delta x_i}{l} \Big|_{\alpha_l \rightarrow 0} & l/2 \leq |x_i| \leq (l+\Delta l)/2 \end{cases} \quad \text{und} \quad \hat{F}_{\text{hom}}(x_i) = \frac{\hat{F}_{\text{hom}} \Delta x_i}{l}$$

Following these conclusions, the calculated membrane velocity is entered as limit value estimation in the diagram of Figure 5. The membrane velocity exceeds the measured initial value by factor 2. By the statistical layout of supporting points of the membrane on the rails, the transducer zones have a local supporting distance of $l+\Delta l$ and each of them has its own resonance frequency. The resonance frequency varies little around the acoustical resonance of the transducer. Hence, the real membrane velocity has a lower value than calculated by equation 3 with a slightly increased bandwidth.

SUMMARY

The sound pressure of multi-stripe membrane transducers with isolating rails is determined by the achievable homogeneous electrical field in the airgap. It is limited, if the increased electric field strength between rails and membrane outruns the disruptive strength. The high sound pressure of transducers with transmitting rails to be recognised at low voltages can not theoretically be understood easily even than considering the inhomogeneous electrical field in the airgap. To explain this effect, the zones between rail surface and membrane will remain, where the vibration energy of the metal-film-connection is fed into the transducer. The network model shows the local assessment of the energetic field with the eigen mode of the membrane. Using this knowledge, the maximum effect of the metal-film-connection was estimated.

With minimised compression loss and constant electrical input conditions, transducers with transmitting rails produce a higher sound pressure than their equivalent with isolating rails.

LIST OF LITERATURE

- [1] Anderson, M. J.; Dogan, N. S.; Hill, J. A.; Fortunko, C. M.; Moore, R. D.: Broadband electrostatic transducers: Modelling and experiments. *Journal of Acoustic Society of America* 97 (1) January 1995
- [2] Haller, M. I.; Khuri-Yakub, B. T.: A Surface Micromachined Electrostatic Ultrasonic Air Transducer. *IEEE Ultrasonics Symposium* 1994; S. 1241 – 1243
- [3] Haller, M. I.; Khuri-Yakub, B. T.: A Surface Micromachined Electrostatic Ultrasonic Air Transducer. *IEEE Transactions on Ultrasonics, Ferroelectrics and Frequency Control* Vol. 43 No. 1 1996
- [4] Hietanen, J.; Stor-Pellinen, J.; Luukkala, M.; Mattila, P.; Tsuzuki, F.; Sasaki, K.: A Helmholtz resonator model for an electrostatic ultrasonic air transducer with a V-grooved backplate. *Sensors and Actuators A*, 39 (1993); S. 129-132
- [5] Jin, X.; Ladabaum, I.; Khuri-Yakub, B. T.: The Microfabrication of Capacitive Ultrasonic Transducers. *Journal of Microelectromechanical Systems* Vol. 7 No. 3 September 1998
- [6] Lenk, A.; Pfeifer, G.; Werthschützky, R.: *Elektromechanische Systeme*. Springer Verlag 2001
- [7] Leschka, S.: Diplomarbeit. TU Dresden 2000; Institut für Akustik und Sprachkommunikation
- [8] Leschka, S.: Resonante kapazitive Ultraschallwandler mit leitenden und isolierenden Stegen. *Fortschritte der Akustik; DAGA 2002; Bochum*
- [9] Leschka, S.; Pfeifer, G.: Resonante kapazitive Ultraschallwandler - Dimensionierung mit Netzwerkmethoden. *Fortschritte der Akustik; DAGA 2001; Hamburg*
- [10] Mattila, P.; Tsuzuki, F.; Väättäjä, H.; Sasaki, K.: Electroacoustic Model for Electrostatic Ultrasonic Transducers with V-Grooved Backplates. *IEEE Transactions on Ultrasonics, Ferroelectrics and Frequency Control*; Vol. 42, No. 1; January 1995
- [11] Rafiq, M.; Wykes, C.: The Performance of Capacitive Ultrasonic Transducers using V-Grooved Backplates. *Measurement, Science and Technology*; Vol. 2, S. 168 - 174; 1991